General features of the energy landscape in Lennard-Jones-like model liquids

L. Angelani
Dipartimento di Fisica, INFM, and SMC-INFM, Università di Roma La Sapienza, P. A. Moro 2, I-00185 Roma, Italy,

G. Ruocco
Dipartimento di Fisica and INFM, Università di Roma La Sapienza, P. A. Moro 2, I-00185 Roma, Italy

M. Sampoli
Dipartimento di Energetica and INFM-Università di Firenze, Via Santa Marta 3, I-50139 Firenze, Italy, and LENS, Via Nello Carrara 1, I-50019 Sesto-Fiorentino, Italy

F. Sciortino
Dipartimento di Fisica, INFM, and SMC-INFM, Università di Roma La Sapienza, P. A. Moro 2, I-00185 Roma, Italy,

(Received 28 February 2003; accepted 7 May 2003)

Features of the energy landscape sampled by supercooled liquids are numerically analyzed for several Lennard-Jones-like model systems. The properties of quasisaddles (minima of the square gradient of potential energy $W=|\nabla V|^2$), are shown to have a direct relationship with the dynamical behavior, confirming that the quasisaddle order extrapolates to zero at the mode-coupling temperature T_{MCT}. The same result is obtained either analyzing all the minima of W or the saddles (absolute minima of W), supporting the conjectured similarity between quasisaddles and saddles, as far as the temperature dependence of the properties influencing the slow dynamics is concerned. We find evidence of universality in the shape of the landscape: plots for different systems superimpose into master curves, once energies and temperatures are scaled by T_{MCT}. This allows to establish a quantitative relationship between T_{MCT} and potential energy barriers for Lennard-Jones-like systems, and suggests a possible generalization to different model liquids. © *2003 American Institute of Physics.* [DOI: 10.1063/1.1587132]

I. INTRODUCTION

The investigation of the topological and metric properties of potential energy surface (PES), often referred to as ''energy landscape,'' is a useful and powerful tool for studying slow dynamics in condensed matter, especially in those cases where the lack of order (as for example in supercooled liquids) inhibits the use of the analytical tools pertaining to the crystalline state.[1–6] The PES approach has been successfully applied to the study of many different interacting systems (glasses, proteins, sheared materials, and so on). The PES approach started with the introduction of the fruitful concept of *inherent structures*.[7] In the last years, several steps toward a more detailed description of the statistical properties of the PES have been performed, most of them pointing toward a better understanding of the relationship between the landscape properties and the emergent dynamical behavior of the analyzed systems.

Among others, two landscape-based approaches have proven to be particularly stimulating. The first one concerns the detailed analysis of the *inherent structures* (i.e., the configurations at the minima of potential energy) visited by the system at different temperatures. This method has allowed to clarify many interesting phenomena, as, for example, the thermodynamic picture of the supercooled liquid regime based on the configurational entropy,[8] the relationship between fragility and properties of inherent structures,[5] the analysis of diffusion processes in terms of visited inherent structures,[6,9,10] or the interpretation of the effective fluctuation-dissipation temperature in the out-of-equilibrium regime in terms of inherent structures visited during aging,[11] only to cite a few. The second approach is based on the analysis of the eigenvalues (normal modes) of the Hessian at the instantaneous configurations during the dynamic evolution of the system, from here the name *instantaneous normal mode approach* (for an introduction and an extended application of this method see the works of Keyes and co-workers[12,13]). This approach allowed to relate the emergent diffusive processes to the features of the landscape, opening the way to the interpretation of diffusion in terms of accessible paths in the multidimensional energy surface. Promising steps were obtained (i) using simultaneously both the instantaneous normal mode approach and the inherent structure one, in order to identify the relevant slow diffusive directions,[14,15] and (ii) by analyzing the reaction paths in order to eliminate the nondiffusive unstable modes.[16]

Recently, a further approach has been introduced[17,18] and applied to the study of supercooled liquids.[19–25] This approach is based on the analysis of the *saddles* of the potential energy surface and has provided new insight in the analysis of the dynamic crossover taking place on lowering the temperature in supercooled liquids. Indeed it allows to characterize the dynamic transition temperature T_{MCT} (mode-

coupling temperature[26]) as the temperature where the order (fractional number of negative eigenvalues of the Hessian matrix) of the saddles vanishes. This finding suggested the following scenario for the dynamics: above T_{MCT} the representative point in the configuration space lies close to the saddles and the relevant dynamic process is the diffusion among multidimensional saddle points, i.e., the diffusion takes place along paths at almost constant potential energy, and the limiting factors to particles diffusion are ''entropic,'' rather than ''energetic,'' barriers. On the contrary, below T_{MCT} the minimum-to-minimum diffusion processes dominate and the ''true'' barrier jump controls the diffusive dynamics. A clear landscape-based interpretation of the dynamic behavior of the system is then provided. It is important to mention here that the term ''saddles'' is not mathematically correct, as the way the saddles have been defined in Refs. 17 and 18 is based on the partition of the configuration space in basins of attraction of the minima of the ''pseudopotential'' [27] $W=|\nabla V|^2$. It is clear that the absolute minima of W, located at $W=0$, are true saddles of the energy surface (for simplicity of notation we call ''saddles'' also the minima and maxima of V) while the local minima of W (those with $W>0$) correspond to points with (at least) one inflection direction, and are not saddles in mathematical sense, rather they are ''shoulders'' along the inflection direction. As pointed out by Doye and Wales,[20] the local minima of W, and not the absolute ones, are very often encountered during the minimization procedure. However, as it will be clear soon, the properties of the local and absolute minima of W which are actually important in determining the diffusive behavior are exactly the same. For this reason we call the local minima of W *quasisaddles*, to emphasize the fact that they carry the same information as saddles, even if they are geometrically different in nature (for a more detailed discussion see Refs. 28–30).

Besides the landscape picture of the dynamic processes, the study of saddles has also permitted a quantitative characterization of the main features of the PES of liquid systems. Indeed, important PES properties, as the mean energy elevation of saddles from underling minima or the Euclidean distances among saddles, can be inferred from the analysis of saddle properties. It emerges an high regularity of the PES, with few parameters describing the spatial and energetic location of saddles.

In this work we apply the saddle-approach to different model liquids (Lennard-Jones-like pair potentials), in order to better understand the relationship between landscape properties and slow dynamics, and in order to evidencing the existence of general features of the PES. The main result of this work is the existence of master curves both for temperature-dependent properties (saddle order versus T) and for landscape properties (saddle energy versus order), once energies and temperatures are normalized to T_{MCT}. This is a very strict relationship between dynamics and landscape features: differences in the PES for different systems simply define different T_{MCT} values, and once scaled by these values, one obtains exactly the same behavior. In other words, it appears that the PESs are very similar, the only differences being the values of few parameters describing them (like the mean elevation barriers ΔE-mean elevation of saddles of order one from underlying minima) that lead to different values of dynamical quantities (T_{MCT}). The last point is of particular importance: for all the systems investigated we obtain that the value of T_{MCT} is about 1/10 of the energy barrier ΔE, suggesting a kind of universality in the rearrangement processes governing the diffusion.

II. MODELS

We numerically investigated four different Lennard-Jones-like model systems, all composed of $N=256$ particles inside a cubic box with periodic boundary conditions. These are:

(1) the modified monatomic Lennard-Jones (MLJ),[31] at $\rho=1.0$ (hereafter all the quantities will be expressed in LJ reduced units)
$$V_{\mathrm{MLJ}}(r)=4\epsilon[(\sigma/r)^{12}-(\sigma/r)^{6}]+\delta V, \quad (1)$$
where δV is a (small) many-body term that inhibits crystallization
$$\delta V=\alpha\Sigma_{\mathbf{q}}\theta(S(\mathbf{q})-S_0)[S(\mathbf{q})-S_0]^2. \quad (2)$$
$S(\mathbf{q})$ is the static structure factor, the sum is made over all $\mathbf{q}$ with $q_{\max}-\Delta<|\mathbf{q}|<q_{\max}+\Delta$, where $q_{\max}=7.12(\rho)^{1/3}$ and $\Delta=0.34$, and the values of the parameters are $\alpha=0.8$ and $S_0=10$.

(2) the modified monatomic soft spheres (MSS), at $\rho=1.0$,
$$V_{\mathrm{MSS}}(r)=4\epsilon(\sigma/r)^{12}+\delta V, \quad (3)$$
where δV is defined in Eq. 2.

(3) the binary mixture Lennard-Jones 80-20 (BMLJ),[32] at density $\rho=1.2$,
$$V_{\mathrm{BMLJ}}(r)=4\epsilon_{\alpha\beta}[(\sigma_{\alpha\beta}/r)^{12}-(\sigma_{\alpha\beta}/r)^{6}], \quad (4)$$
where the values of the parameters are those of the Kob-Andersen mixture ($\sigma_{AA}=1$, $\sigma_{AB}=0.8$, $\sigma_{BB}=0.88$, $\epsilon_{AA}=1$, $\epsilon_{AB}=1.5$, $\epsilon_{BB}=0.5$);

(4) a variant of the binary mixture Lennard-Jones (BMLJ_2), at $\rho=1.2$, in which the values of σ_{AA} and σ_{BB} were exchanged.

In the case of BMLJ and BMLJ_2, the interaction potential is tapered at long distances between $r_1=2.43\sigma_{AA}\leqslant r\leqslant 2.56\sigma_{AA}=r_2$ with the following fifth-order smoothing function $\mathcal{T}(r)=1+(r_1-r)^3(6r^2+(3r+r_1)(r_1-5r_2)+10r_2^2)/(r_2-r_1)^5$. In this way the potential, the forces and their derivatives are continuous, the energy can be kept constant to better than $1/10^5$ over 100 millions of time steps. The MLJ and MSS potential have been simply cut and shifted at 2.5σ.

We performed standard molecular dynamics simulations at equilibrium (*NVE* ensemble), in a temperature range from $T=2$ down to the lowest temperature that can be equilibrated in the MD run (this temperature is strongly model dependent). Along the equilibrium molecular dynamics trajectories at a given temperature we analyzed the properties of (i) the instantaneous configurations; (ii) the inherent structures (minima); and (iii) the saddle configurations. About 1000 configurations have been analyzed for each temperature and for each system. The inherent structures associated to instantaneous configurations are obtained by a conjugate-gradient

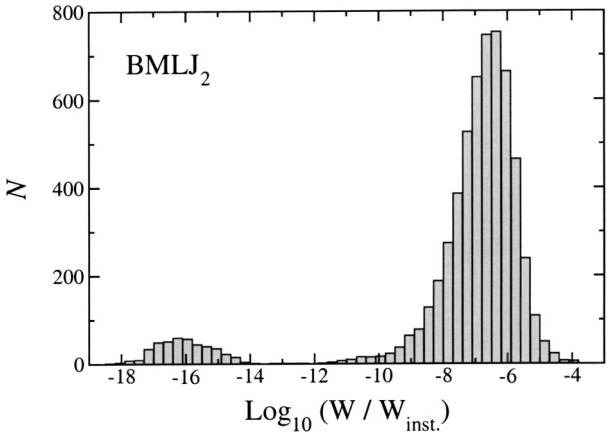

FIG. 1. Histogram of the ratio $W/W_{\text{inst,}}$, i.e., the value at the minima of W with respect to the value at instantaneous configurations, at $T=2$ for $BMLJ_2$ (6000 configurations analyzed). The higher region corresponds to quasisaddles (local minima of W), while the lower one to true saddles (absolute minima).

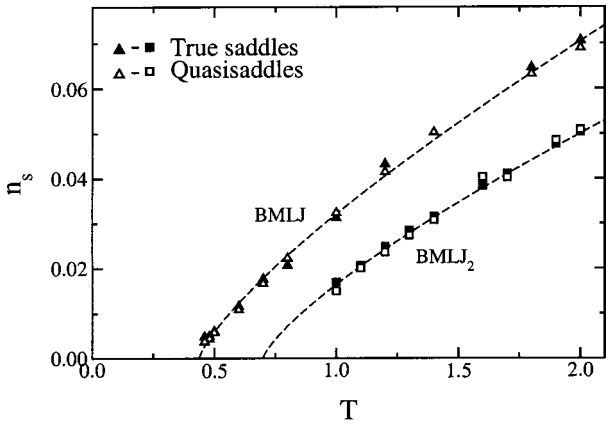

FIG. 2. Temperature dependence of the fractional order of true saddles (full symbols) and quasisaddles (open symbols), for BMLJ (triangles) and $BMLJ_2$ (squares). Dashed lines are power law fits.

minimization procedure on the total potential energy. For saddles, a similar minimization procedure has been applied to the pseudo-potential $W=|\nabla V|^2$. The tapering of the BMLJ and $BMLJ_2$ potentials allows the minimization procedures of both V and W to work correctly as they are not affected by small discontinuities in the derivative of V and W. The importance of avoiding discontinuities in order to obtain good W minimization has been recently underlined in Ref. 23 where the LBFGS algorithm[33] was used. However to obtain good minimizations of W, even for a ''small'' system of 256 particles (i.e., 768 dimensions), is a stiff problem. We tested different minimization algorithms (steepest-descent, Gauss-Newton, preconditioned conjugate gradient, Levenberg-Marquardt[34]) but they eventually stick in some points of the configuration space, where the algorithm decrease more and more the step size, and the search becomes inefficient and possibly stops. Different algorithms usually stick in different points. Sometimes the same algorithm who stuck in a given point can be effective in overcoming the critical situation if a larger step is used. Therefore, in the present work, a complex flow chart with various algorithms was used to obtain good minima (the details of the numerical algorithms will be presented elsewhere[35]). We want to remark that in this way the calls to the function W are always less than 3500 (average$\approx$1500) and less than 1000 (average$\approx$200) to the derivative of W.

For all the analyzed configuration points (instantaneous, minima and saddles) we store the energies per particle (e, e_{IS}, and e_s respectively), and for instantaneous and saddles we also determine their order n and n_s, defined as the fractional number of negative eigenvalues of the Hessian, i.e., the absolute number of negative curvatures over $3N$ (for inherent structures one obviously has $n_{IS}=0$).

III. SADDLES AND QUASISADDLES

First of all we focus our attention on the differences between saddles (absolute minima of W) and quasisaddles (local minima of W). As an example, Fig. 1 shows, for the case of $BMLJ_2$ model, the histogram of the value of the pseudopotential W at the minima (6000 configurations analyzed at $T=2$). The values of W at the minima are normalized to the values at the corresponding instantaneous configurations, i.e., to the value of W before starting the W-minimization procedure. We observe two very well distinct regions: the one with higher W values corresponds to local minima of W (quasisaddles), the lower one corresponds to absolute minima (true saddles). The non-zero values of W on the low-W peak is due to the finite precision and/or threshold employed in the minimization procedure. A closer inspection of the eigenvalues of the Hessian shows that the quasisaddles are points with only one extra zero eigenvalue[29] (besides the three connected to the global translations), corresponding to an inflection one-dimensional profile along the corresponding eigenvector. The fact that in the plot the two regions are well separated, allows to discriminate true and false saddles in a clear way. On the contrary, no clear separation has been found between saddles and quasisaddles from the analysis of the eigenvalues: due to the finite precision the found eigenvalues relative to the inflection points are different from zero of the same amount of the lowest frequency eigenvalues of real vibrational (or diffusive) modes. As it is evident from Fig. 1, true-saddles are very few and their number are found to decrease on lowering the temperature (e.g., for $BMLJ_2$ in Fig. 1 about 5% at $T=2$, and for BMLJ about 2% at $T=2$ and less than 1% at $T=0.48$).

An interesting observation arises from the analysis of the behavior of the T-dependence of the number of negative curvatures in the ''true'' saddles and in the quasisaddles separately. In Fig. 2 the saddle order is shown as a function of the temperature using only the true- (full symbols) and the quasi- (open symbols) saddles, for the cases of BMLJ (triangles) and $BMLJ_2$ (squares) models (we note that in the $BMLJ_2$ case, due to the appearance of crystallization, the data are available only for $T\gtrsim 1$). The coincidence between the two set of data indicates that, as far as the temperature dependence of their characteristics (order and energy) is concerned, quasisaddles and true saddles share the same properties. Also other properties, as for example the spectral features (i.e., the density of vibrational states), of quasi-

TABLE I. For the different Lennard-Jones-like models we report the investigated density ρ, the mode-coupling temperature T_{MCT} (estimated from the apparent power-law vanishing of the diffusion coefficient), the mean barrier values ΔE (mean elevation of order-one saddles from underlying minima) and the reduced barrier height $\Delta E^* = \Delta E / T_{MCT}$. All the quantities are in LJ reduced units.

Models	ρ	T_{MCT}	ΔE	ΔE^*
MLJ	1.0	0.475	4.43	9.3
MSS	1.0	0.210	2.06	9.8
BMLJ	1.2	0.435	4.16	9.6
$BMLJ_2$	1.2	0.605	5.93	9.8

saddles and true-saddles are found indistinguishable.[25] This finding suggests that, no matter if saddles or quasisaddles, the minimization of W leads to points of the PES that are relevant for a landscape-based interpretation of the slow dynamics of the system: the order extrapolates to zero at the mode-coupling temperature T_{MCT} (see Table I for the values of T_{MCT}, estimated from diffusivity data, for the different models), indicating that at this temperature the properties of the landscape probed by the system manifest a kind of discontinuity (the number of open directions, related to the saddle order, goes to zero and the dynamical processes change their characteristics). In other words, the minimization of W seems to be a good method to get ride of the fast degrees of freedom and to keep information only on the slow degrees relevant for the slowing down of the dynamics taking place in supercooled regime.

IV. GENERAL FEATURES OF THE PES

We now turn our attention to the existence of common features among the different model systems analyzed.

A. *T*-dependent properties

As already pointed out in Refs. 17 and 28, the (quasi-) saddle order, n_s, vanishes as T approaches T_{MCT} from above. At a first sight, it seems that the specific behavior of $n_s(T)$ is a model-dependent property (see Fig. 2). However, we observe that after the scaling the temperature scale by a specific sample dependent quantity, i.e., by T_{MCT}, all the models behave similarly. In Fig. 3 the saddle order n_s is reported as a function of reduced temperature T/T_{MCT}. All the curves for the different systems collapse into a single master curve. The latter can be fitted by a power law

$$n_s = \overline{n}\left(\frac{T}{T_{MCT}} - 1\right)^{\gamma}, \tag{5}$$

with $\gamma = 0.85$ and $\overline{n} = 0.025$ (in the fitting procedure, the values of T_{MCT}, reported in Table I, are kept fixed to the ones derived by the fit of the power-law behavior of the diffusion coefficient). A similar master plot is obtained also for the relation between the saddle energy and the temperature. These results suggest a universal behavior (at least for the LJ-like model systems analyzed here): at a given reduced temperature $T^* = T/T_{MCT}$ all the systems visit saddles with the same properties (hereafter we will indicate with "*" the temperature and the energy scaled by T_{MCT}). One could conjecture that this universality is due to the repulsive part of the pair potential r^{-12} (common to all the systems), that dominates over the attractive one at the studied densities. However, the facts that the curves superimpose each other quite well in the whole temperature range and that non-LJ systems (as, for example, the Morse potential—see the next section) show a similar behavior, seems to indicate that the observed universality is not trivially related to the repulsive part of the interaction potential. Finally, we want to remark that the small value of $\overline{n}$ indicates that even at temperature twice that of the MCT critical point, the system is visiting saddles of low order ($n_s \simeq 0.025$), so indicating that at $T = 2T_{MCT}$ the closest saddle, according to the partitioning defined by the minimization of W, is far below the top of the landscape.

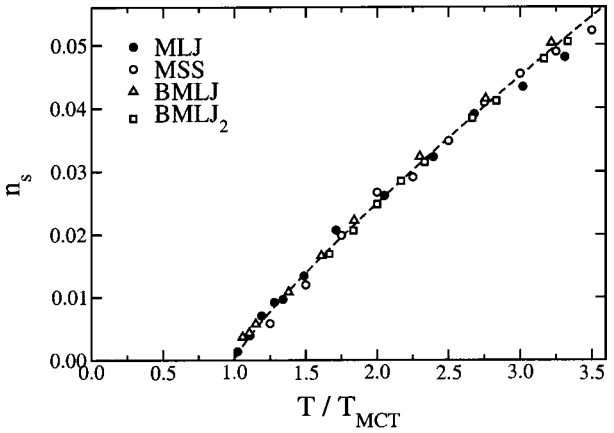

FIG. 3. Saddle order n_s as a function of reduced temperature T/T_{MCT}, for all the analyzed systems. The dashed line is a power law with exponent $\gamma = 0.85$. For MLJ and MSS $\rho = 1.0$, while for BMLJ and $BMLJ_2$ $\rho = 1.2$.

B. Energy barriers and T_{MCT}

The existence of common and general features of the PES emerges in a clear way from the comparative analysis of the energy and of the order of the saddles. In Fig. 4 part A the energy elevation $\Delta e_s = e_s - e_{IS}$ of the saddles from the underling minima is plotted as a function of the saddle order n_s for the different investigated models. As already observed,[17] there exists a proportionality between these two quantities, indicating a simple organization of the PES: saddles are equally spaced in energy over the minima. The slopes of the different straight lines in Fig. 4 determine the elementary energy elevation ΔE of saddles of order n from saddles of order $n-1$:

$$\Delta E = \frac{1}{3}\frac{d(e_s - e_{IS})}{dn_s}, \tag{6}$$

where the factor 3 is due to the fact that energies are per particles (N) and the fractional order per degrees of freedom ($3N$). The values of ΔE obtained for the various systems are reported in Table I. A possible explanation of the linear relationship observed in Eq. 6 is that there exist in the system several spatially uncorrelated rearranging regions, each experiencing a mean barrier energy ΔE. In other words, if the system as a whole lies on a saddle of order m, this is due to the fact that there are m uncorrelated subsystems each one visiting a saddle of order 1. The analysis of the specific

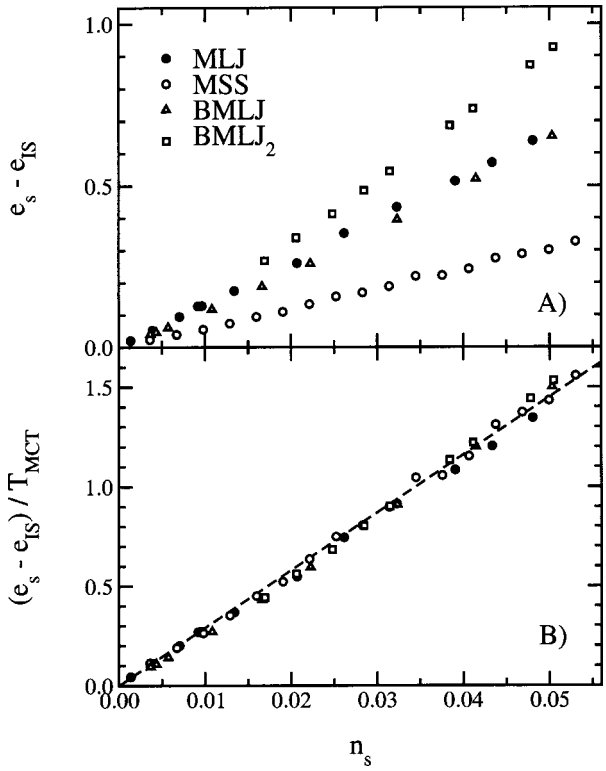

FIG. 4. (A) Energy elevation of saddles from underling minima $e_s - e_{IS}$ against saddle order n_s; (B) Energy elevation rescaled by mode-coupling temperature T_{MCT} against saddle order n_s. Dashed straight line is a guide to the eyes.

atomic motion associated to these saddles, needed to assess or disprove the validity of this hypothesis, is beyond the aim of the present work.

A very interesting and surprising result is obtained by scaling the energy values reported in Fig. 4 part A to the mode-coupling temperature T_{MCT} ($K_B=1$), obtaining again a single master curve (see Fig. 4 part B). The landscapes of different systems seem to share common features, with only one parameter describing the organization of saddles, i.e., the mean elevation ΔE, that becomes an universal parameter ($\Delta E^* = \Delta E / T_{MCT} \simeq 9 \div 10$) once normalized to the mode-coupling temperature (see the last column of Table I). In other words, all the models have the common property that the elementary barrier height is about 10 times the critical temperature T_{MCT}:

$$\Delta E \simeq 10 \ T_{MCT}. \tag{7}$$

This relation have been numerically proved for the four potential models investigated here. The same relation also holds for another LJ-like model, the binary mixture soft-sphere model (BMSS) investigated in Ref. 24 (at $\rho=1$). This observation gives further support to the universality of Eq. 7. If this is a particular characteristic of Lennard-Jones-like models or a general feature of a more wide class of simple liquids is a open and interesting question which remains to be answered.

We can try to give a first answer to this question analyzing the available data in the literature for other systems. To our knowledge, besides the Lennard-Jones-like systems, a saddle-based analysis has been performed only for the Morse potential.[22] The Morse potential, used in Ref. 22, is defined as $V_\alpha(r) = \epsilon[1 - \exp(\alpha(1 - r/r_e))]^2 - \epsilon$, where ϵ is the well depth, r_e is the interparticle distance, and the parameter α is inversely correlated to the range of the potential. Differently from soft-spheres and LJ, the Morse potential is finite as $r \to 0$. Unfortunately, equilibrium simulation based on the Morse potential are difficult, since the undercooled system crystallizes easily. Therefore simulations reported in Ref. 22 have been performed only well above T_{MCT}. It was found that the larger the value of α is, the further the distance between the temperature of the lowest noncrystalline simulation and T_{MCT} is. In this study, a linear dependence between n_s and e_s have been observed and the values of de_s/dn_s normalized to T_{MCT} are in agreement with Eq. 7 for the three smaller α values $\alpha=4$, 5, and 6 (ΔE^* are in the range $9.3 \div 10.5$[36]). For the two highest α values, $\alpha=9$ and 12, the reported values for ΔE^* are quite different (4.6 and 3.5, respectively). Further studies, for example focussing on binary mixture systems, are requested to find out if such discrepancy is due to an approximate determination of T_{MCT} for $\alpha=9$ and 12 (which was obtained by extrapolating $n_s(T)$ from a temperature region where n_s is far away from zero, $n_s(T) \gtrsim 0.2$). Uncertainties in the estimates of T_{MCT} at large α are also consistent with the unexpected nonmonotonic dependence of T_{MCT} with α reported in Ref. 22. We conclude that, for all α values for which the reliability of the data is unquestionable, the Morse potential landscape shares the same characteristic of those of the LJ-like potentials.

In all the other model systems studied in the literature we do not have a direct information on the saddle energy elevation. However, the existence of a well defined barrier energy scale ΔE in the PES is expected to control the activation processes at low temperature, giving rise to an Arrhenius behavior of the transport properties at temperatures below T_{MCT}. The existence of Arrhenius law in LJ-like systems—that are basically ''fragile,'' in the Angell classification scheme[2]—would be, per se, surprising (however, the degree of fragility of LJ systems is a matter of debate[37]).

The simulations below T_{MCT} are very difficult to perform, due to the extremely long relaxation times in this regime and a direct inspection of the expected Arrhenius behavior is not easy to pursuit. Only very recently such a kind of analysis has been performed for the BMLJ model at $\rho=1.2$.[38] In that work an Arrhenius behavior was actually found in the temperature dependence of the diffusion coefficient below T_{MCT}: $D \propto \exp(-\Delta E_{Arr}/T)$ (we use the symbol ΔE_{Arr} for the activation energy in the Arrhenius law of the diffusivity, to distinguish it from the energy barrier ΔE determined from the saddles analysis of the PES), with a value of $\Delta E_{Arr} \simeq 8.1$. The observed Arrhenius behavior is somewhat surprising in this ''fragile'' liquid models, and seems to indicate that close to T_{MCT} activated processes start to be relevant and dominate the dynamics. However, the value of the activation energy ΔE_{Arr} found in Ref. 38 is not equal to the elementary barrier energy ΔE estimated from the saddles analysis (see Table I), but it is about twice that value: $\Delta E_{Arr}/\Delta E \simeq 1.9$. Re-analyzing our data for the MLJ model (for which we have few thermodynamic points equilibrated

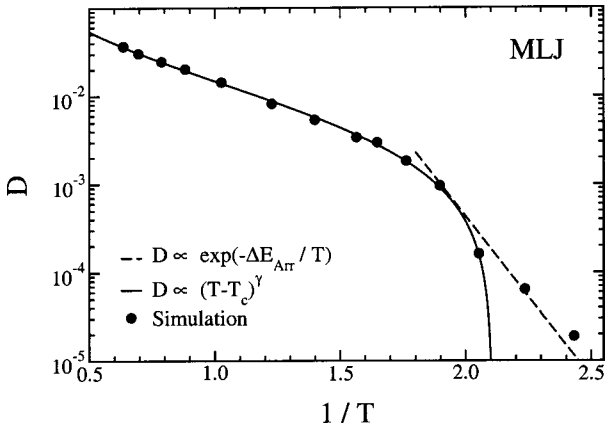

FIG. 5. Diffusivity D as a function of inverse temperature $1/T$ for the MLJ model. Straight line represents the mode coupling like power law fit. Dashed line is the Arrhenius law with energy barrier $\Delta E_{Arr} \simeq 1.9 \Delta E = 8.4$ (ΔE is the energy barrier from saddles—see Table I), following the corresponding relation obtained for the BMLJ case (Ref. 38).

TABLE II. Reduced energy barrier heights estimated from saddles ($\Delta E^* = \Delta E / T_{MCT}$) and from low-temperature Arrhenius law of diffusivity ($\Delta E^*_{Arr} = \Delta E_{Arr} / T_{MCT}$) for different model systems. The data of MLJ, MSS, BMLJ, and $BMLJ_2$ are from this work (except the ΔE^*_{Arr} for BMLJ, that is from Ref. 38).

Models	ΔE^*	ΔE^*_{Arr}
MLJ	9.3	17.7
MSS	9.8	...
BMLJ	9.6	18.6[a]
$BMLJ_2$	9.8	...
BMSS[b]	9.1	...
Morse[c]	9.3÷10.5	...
Silica (BKS)[d]	...	16÷18
OTP[e]	...	20÷28
Water (SPC/E)[f]	...	40

[a]Reference 38.
[b]Reference 24.
[c]Reference 21 (obtained for $\alpha = 4, 5, 6$).
[d]Reference 41.
[e]Reference 42.
[f]Reference 43.

close to but below T_{MCT}), we find that the above reported ratio is compatible with MLJ data (see Fig. 5), even if statistic is poorer than that of BMLJ case and the equilibrium condition is not fully satisfied by the lowest two temperature points. If such observation has general validity, then Arrhenius behavior should be observed below T_{MCT}, with an activation energy value about 2 times the value of the elementary saddle energy barrier [so obtaining a value of reduced barrier energy (normalized to T_{MCT}) $\Delta E^*_{Arr} \simeq 18 \div 20$]. The origin of this factor two needs to be further clarified. To this aim, it is important to underline that the ''effective'' energy barriers for activated processes as seen by the dynamics (i.e., those entering in the Arrhenius law for the diffusivity) can be higher than the minimum-to-saddle energy difference (as measured directly by analyzing the PES). This can be due to the fact that the true diffusive path in the landscape[39] could pass higher in energy with respect to the saddle point, in order, for example, to minimize the minimum-to-minimum path length (i.e., for entropic reasons). In this respect, it is worth to mention that a noncoincidence between the relaxation times determined either through MD simulations or through the direct inspection of the PES has been observed in the simulation of a model protein during the folding process.[40] In particular, the results in Ref. 40 indicates that the effective saddle height is larger than the actual one.

Having in mind that $\Delta E^*_{Arr} \simeq 2 \Delta E^*$ and that $\Delta E^* \simeq 10$ (i.e., $\Delta E^*_{Arr} \simeq 20$), we can try to analyze what is observed for other model potentials existing in the literature where the $D(T)$ has been determined. We found three different models for which a low temperature analysis of $D(T)$ has been performed *via* molecular dynamics: (i) The BKS-silica model,[41] for which the values of ΔE^*_{Arr} are 16.2 and 18.0, for the self-diffusion of O and Si, respectively; (ii) the Lewis and Wahnström ortho-terphenyl model,[42] for which the temperature dependence of the molecular center of mass diffusion coefficient at five different densities give values of reduced barrier energy $\Delta E^*_{Arr} \simeq 20 \div 28$ (except the lowest density that gives a value of about 10); (iii) The SPC/E-water model,[43] for which one finds $\Delta E^*_{Arr} \simeq 40$. Table II summarizes the known results on energy barrier heights estimated from saddles and from Arrhenius low-temperature dependence of diffusivity. The values for MLJ, MSS, BMLJ, and $BMLJ_2$ are from the present work, except the ΔE^*_{Arr} for BMLJ that is obtained from Ref. 38. In future works we will try to determine the saddle-barriers ΔE^* for non-LJ systems (the last three systems in the table), in order to have a better understanding of the diversity of the different landscapes. In conclusion, besides the case of water, the other systems seem to be in agreement with the findings of this work (the values of the reduced barrier energies are of the same order), evidencing a quite general universality of the observed relations. A deeper understanding of the differences among various model liquids deserves further investigations.

V. CONCLUSIONS

In conclusion, despite complex and disordered in nature, the simple liquid PES seems to exhibit few general and regular features, useful both to bring important insight for the understanding of the relevant diffusion processes taking place in supercooled liquids and to construct simplified PES models. The main findings of the present work can be summarized as:

- the coincidence between the temperature dependence of the quasisaddles and of the true saddles properties;
- the existence of master curves for saddle properties, once energies and temperatures are rescaled by the mode coupling critical temperature T_{MCT};
- the existence of a universal relationship between the mode-coupling temperature and the mean energy barrier height $\Delta E \simeq 10\, T_{MCT}$, that seems to extend beyond the class of the Lennard-Jones-like models analyzed here.

Finally, we would like to point out that it already exists in the literature an hint on the existence of a linear relationship between ΔE_{Arr} and the mode coupling critical temperature. Indeed, in a large class of glassy system one experimentally observes a linear relationship between the glass

transition temperature T_g and the infinite-frequency shear modulus G_∞:[44] $T_g \propto G_\infty$. If we use the findings of our work ($\Delta E^*_{Arr} \simeq 10$, i.e., $\Delta E_{Arr} \simeq 10\, T_{MCT}$) and we allow ourselves to confuse T_g with T_{MCT}, the following relation emerges: $\Delta E_{Arr} \propto G_\infty$. This relation is the prescription of the ''shoving model'' introduced thirty years ago by Nemilov[45] and recently put in a more rigorous form by Dyre *et al.*[46] The validity of the proportionality between ΔE_{Arr} and G_∞ has been proved for different glasses, and, together with the linear relationship between T_g and G_∞, give further support to the finding of the present work, i.e., the apparent universality of the ratio $\Delta E_{Arr}/T_{MCT}$.

ACKNOWLEDGMENTS

We acknowledge support from INFM, PRA GenFDT, MURST COFIN2002, and FIRB. G.R. thanks J.C. Dyre for useful discussions.

[1] P. G. Debenedetti and F. H. Stillinger, Nature (London) **410**, 259 (2001).
[2] C. A. Angell, Science **267**, 1924 (1995).
[3] S. Sastry, P. G. Debenedetti, and F. H. Stillinger, Nature (London) **393**, 554 (1998).
[4] S. Büchner and A. Heuer, Phys. Rev. Lett. **84**, 2168 (2000).
[5] S. Sastry, Nature (London) **409**, 164 (2001).
[6] T. Keyes and J. Chowdhary, Phys. Rev. E **65**, 041106 (2002).
[7] F. H. Stillinger and T. A. Weber, Science **225**, 983 (1984); F. H. Stillinger, *ibid.* **267**, 1935 (1995).
[8] F. Sciortino, W. Kob, and P. Tartaglia, Phys. Rev. Lett. **83**, 3214 (1999); E. La Nave, S. Mossa, and F. Sciortino, *ibid.* **88**, 225701 (2002).
[9] G. Fabricius and D. A. Stariolo, Phys. Rev. E **66**, 031501 (2002).
[10] L. Angelani, G. Parisi, G. Ruocco, and G. Viliani, Phys. Rev. Lett. **81**, 4648 (1998).
[11] F. Sciortino and P. Tartaglia, Phys. Rev. Lett. **86**, 107 (2001).
[12] T. Keyes, J. Phys. Chem. **101**, 2921 (1997).
[13] T. Keyes, J. Chem. Phys. **103**, 9810 (1995); T. Keyes, G. V. Vijayadamodar, and U. Zurcher, *ibid.* **106**, 4651 (1997); W. X. Li and T. Keyes, *ibid.* **111**, 5503 (1999); T. Keyes, J. Chowdhary, and J. Kim, Phys. Rev. E **66**, 051110 (2002).
[14] C. Donati, F. Sciortino, and P. Tartaglia, Phys. Rev. Lett. **85**, 1464 (2000).
[15] E. La Nave, A. Scala, F. W. Starr, H. E. Stanley, and F. Sciortino, Phys. Rev. E **64**, 036102 (2001); E. La Nave, H. E. Stanley, and F. Sciortino, Phys. Rev. Lett. **88**, 035501 (2002).
[16] S. D. Bembenek and B. B. Laird, J. Chem. Phys. **104**, 5199 (1996).
[17] L. Angelani, R. Di Leonardo, G. Ruocco, A. Scala, and F. Sciortino, Phys. Rev. Lett. **85**, 5356 (2000).
[18] K. Broderix, K. K. Bhattacharya, A. Cavagna, A. Zippelius, and I. Giardina, Phys. Rev. Lett. **85**, 5360 (2000).
[19] J. Chowdhary and T. Keyes, Phys. Rev. E **65**, 026125 (2002).
[20] J. P. K. Doye and D. J. Wales, J. Chem. Phys. **116**, 3777 (2002).
[21] P. Shah and C. Chakravarty, J. Chem. Phys. **115**, 8784 (2001).
[22] P. Shah and C. Chakravarty, Phys. Rev. Lett. **88**, 255501 (2002).
[23] P. Shah and C. Chakravarty, J. Chem. Phys. **118**, 2342 (2003).
[24] T. S. Grigera, A. Cavagna, I. Giardina, and G. Parisi, Phys. Rev. Lett. **88**, 055502 (2002).
[25] M. Sampoli, P. Benassi, R. Eramo, L. Angelani, and G. Ruocco, J. Phys.: Condens. Matter **15**, S1227 (2003).
[26] W. Götze, J. Phys.: Condens. Matter **11**, A1 (1999).
[27] T. A. Weber and F. H. Stillinger, Phys. Rev. B **31**, 1954 (1985).
[28] L. Angelani, R. Di Leonardo, G. Ruocco, F. Sciortino, and A. Scala, J. Chem. Phys. **116**, 10297 (2002).
[29] J. P. K. Doye and D. J. Wales, J. Chem. Phys. **118**, 5263 (2003).
[30] L. Angelani, R. Di Leonardo, G. Ruocco, F. Sciortino, and A. Scala, J. Chem. Phys. **118**, 5265 (2003).
[31] R. Di Leonardo, L. Angelani, G. Parisi, and G. Ruocco, Phys. Rev. Lett. **84**, 6054 (2000).
[32] W. Kob and H. C. Andersen, Phys. Rev. Lett. **73**, 1376 (1994).
[33] D. C. Liu and J. Nocedal, Math. Program. **45**, 503 (1989).
[34] W. H. Press, B. P. Flannery, S. A. Teukolsky, and W. T. Vetterling, *Numerical Recipes in Fortran* (Cambridge University Press, Cambridge, 1990).
[35] M. Sampoli, to be published. Even the complex flow chart adopted for W minimizations does not guarantee that the configurational point be an absolute or local minimum of W and a check has to be performed in any case.
[36] The data are obtained from Table I in Ref. 22, dividing the values in the second column by a factor 3, for the same reason as reported in the text—see Eq. (6).
[37] C. A. Angell, B. E. Richards, and V. Velikov, J. Phys.: Condens. Matter **11**, A75 (1999).
[38] S. S. Ashwin and S. Sastry, J. Phys.: Condens. Matter **15**, S1253 (2003).
[39] F. Demichelis, G. Viliani, and G. Ruocco, Phys. Chem. Commun. **5**, 1 (1999).
[40] L. Bongini, R. Livi, A. Politi, and A. Torcini (unpublished).
[41] J. Horbach and W. Kob, Phys. Rev. B **60**, 3169 (1999).
[42] S. Mossa, E. La Nave, H. E. Stanley, C. Donati, F. Sciortino, and P. Tartaglia, Phys. Rev. E **65**, 041205 (2002).
[43] F. W. Starr, F. Sciortino, and H. E. Stanley, Phys. Rev. E **60**, 6757 (1999).
[44] S. V. Nemilov, *Thermodynamics and Kinetic Aspects of the Vitreous State* (CRC, Boca Raton, FL, 1995).
[45] S. V. Nemilov, J. Phys. Chem. **42**, 726 (1968).
[46] J. C. Dyre, N. B. Olsen, and T. Christensen, Phys. Rev. B **53**, 2171 (1996); J. C. Dyre and N. B. Olsen, cond-mat/0211042.